KCL-PH-TH/2016-71, DCPT/16/222, IPPP/16/111

# A Boost to $h \to Z\gamma$: from LHC to Future $e^+e^-$ Colliders

Jose Miguel No[1,2] and Michael Spannowsky[3]

[1] *Department of Physics, King's College London, Strand, WC2R 2LS London, UK*
[2] *Department of Physics and Astronomy, University of Sussex, Brighton BN1 9QH, UK*
[3] *Institute of Particle Physics Phenomenology, Physics Department, Durham University, Durham DH1 3LE, UK*

(Dated: December 21, 2016)

A precise measurement of the Higgs $h \to Z\gamma$ decay is very challenging at the LHC, due to the very low branching fraction and the shortage of kinematic handles to suppress the large SM $Z\gamma$ background. We show how such a measurement would be significantly improved by considering Higgs production in association with a hard jet. We compare the prospective HL-LHC sensitivity in this channel with other Higgs production modes where $h$ is fairly boosted, e.g. weak boson fusion, and also to the potential $h \to Z\gamma$ measurement achievable with a future $e^+e^-$ circular collider (*fcc-ee*). Finally, we discuss new physics implications of a precision measurement of $h \to Z\gamma$.

arXiv:1612.06626v1 [hep-ph] 20 Dec 2016

The $h \to Z\gamma$ decay of the Higgs boson constitutes a very challenging collider measurement. Current LHC constraints from ATLAS and CMS with $7-8$ TeV Run 1 data are very weak [1, 2], and projections for the HL-LHC with an integrated luminosity $\mathcal{L} = 3000$ fb$^{-1}$ yield a relative uncertainty on the $h \to Z\gamma$ signal strength of at least $\Delta\mu/\mu \sim 0.3$ [3, 4]. This is much worse than the projected precision in $h \to W^+W^-$, $ZZ$, $\gamma\gamma$, and also significantly less precise than projections for the fermionic Higgs decays $h \to b\bar{b}$, $\tau^+\tau^-$, $\mu^+\mu^-$.

The main reason behind this poor sensitivity is the very low Higgs branching ratio (BR) in the Standard Model (SM) BR$(h \to \ell^+\ell^-\gamma) \simeq 10^{-4}$, together with the shortage of kinematic handles in an inclusive search to efficiently suppress the large SM $(Z \to \ell^+\ell^-)\gamma$ background. Consequently, attempts to measure BR$(h \to Z\gamma)$ in inclusive Higgs production (i.e. without relying on the presence of additional jets) suffer from a small signal-to-background ratio $S/B < 10^{-2}$ [3] and have to rely on a very large integrated luminosity, as foreseen for the HL-LHC, to allow for data-driven background estimates that ameliorate the effect of systematic background uncertainties in presence of small $S/B$.

In this letter we show that it is possible to significantly improve on the precision for this measurement at the LHC by considering Higgs production in association with a hard jet. We detail the kinematical advantages this entails in terms of signal to background discrimination, and compare the projected sensitivity with the one obtained via other Higgs production modes, particularly weak boson fusion (WBF). We further compare the achievable precision in determining BR$(h \to Z\gamma)$ at the HL-LHC with that of a future $e^+e^-$ circular collider (hereinafter *fcc-ee*), which would benefit from a very large amount of integrated luminosity while on the other hand providing a smaller $e^+e^- \to Zh$ Higgs production cross section. We also briefly comment on the prospect of such a precision measurement at a 100 TeV proton-proton collider (hereinafter *fcc-pp*), where using the $h$+jet Higgs production analyzed in this work would be most effective.

Finally, we discuss potential implications of a precision $h \to Z\gamma$ measurement for new physics beyond the SM. In particular, we show the potential gain of studying the decays $h \to \gamma\gamma$ and $h \to Z\gamma$ in concert to probe the quantum numbers of new charged particles that couple to the Higgs boson, in a rather model-independent way.

## Boosting $h \to Z\gamma$ with Jets at the LHC

### *(i) Higgs production in association with a hard jet*

We here focus on the production process $pp \to h\,j$ with the subsequent Higgs decay $h \to (Z \to \ell^+\ell^-)\gamma$, aiming to exploit the characteristic decay pattern of a resonance to separate the small signal from the large SM background. As the signature consists of a jet, two charged leptons and a photon, the entire final state can be reconstructed using objects with small fake rates. Thus, reducible backgrounds are rendered negligible and the only relevant SM background process to consider is $Z\gamma$+jets [1, 2].

The production of $h$ in association with a boosted jet in the present context provides two major kinematical advantages as compared to the inclusive search: *(i)* While for the signal the invariant mass $m_{\ell\ell\gamma}$ distribution peaks around $m_h \simeq 125$ GeV irrespectively of the transverse momentum of the extra jet $p_T^j$, for the background the two variables are correlated and $m_{\ell\ell\gamma}$ shifts to larger values as $p_T^j$ increases, moving away from the signal. *(ii)* A rather soft photon is expected for the SM background as it dominantly comes from initial state radiation. This is mildly independent of the value of $p_T^j$. In contrast, for the signal the values of $p_T^j$ and $p_T^\gamma$ are highly correlated, as $\gamma$ inherits part of the large Higgs boost in events with a hard jet. These two effects, highlighted in Figure 1, allow to significantly improve the sensitivity to $h \to Z\gamma$, as shown below.

We generate the SM signal and background using MadGraph_aMC@NLO [5] including finite top mass effects and showering the partonic process with Pythia 8 [6]. Both signal and background are normalized to their NLO cross section values using a flat $k$-factor, $k = 2.0$ for the signal [7] (see also [8]) and $k = 1.5$ for the background [9]. For event selection we require two isolated

leptons with $p_T^\ell > 10$ GeV, $|y_\ell| < 2.5$ and one isolated photon with $p_T^\gamma > 20$ GeV, $|y_\gamma| < 2.5$. Leptons (photons) are considered isolated if the hadronic energy deposit within a cone of size $R = 0.3$ is smaller than 10% of the $p_T$ of the lepton (photon) candidate. Jets are defined using the anti-$kT$ recombination algorithm with $R = 0.4$, with $p_T^j \geq 50$ GeV and $|y_j| \leq 4.5$.

With two charged isolated leptons and a photon the final state has a high trigger efficiency. To reconstruct the Higgs and $Z$ bosons we further require 80 GeV $\leq m_{\ell\ell} \leq$ 100 GeV and 115 GeV $\leq m_{\ell\ell\gamma} \leq$ 135 GeV. As the invariant masses in the case of the signal are insensitive to the boost of $h$ and $Z$ bosons, analyzing the effect of an increasing jet $p_T^j$ on the the shape of the $m_{\ell\ell\gamma}$ background distribution will help improving the signal-to-background ratio $S/B$. We perform a varying selection on $p_T^{j_1}$ ($j_1$ being the leading jet in transverse momentum in the event), requiring $p_T^{j_1} > p_T^{j_{cut}}$ with three reference $p_T^{j_{cut}}$ values $p_T^{j_{cut}} = 50, 100, 180$ GeV. After selection cuts, these yield rather small event rates, as shown in Table I. We observe that increasing the value of $p_T^{j_{cut}}$ from 50 to 180 GeV improves $S/B$ from 0.7% to 2.3%, but at the expense of reducing the statistical significance measured in $S/\sqrt{B}$.

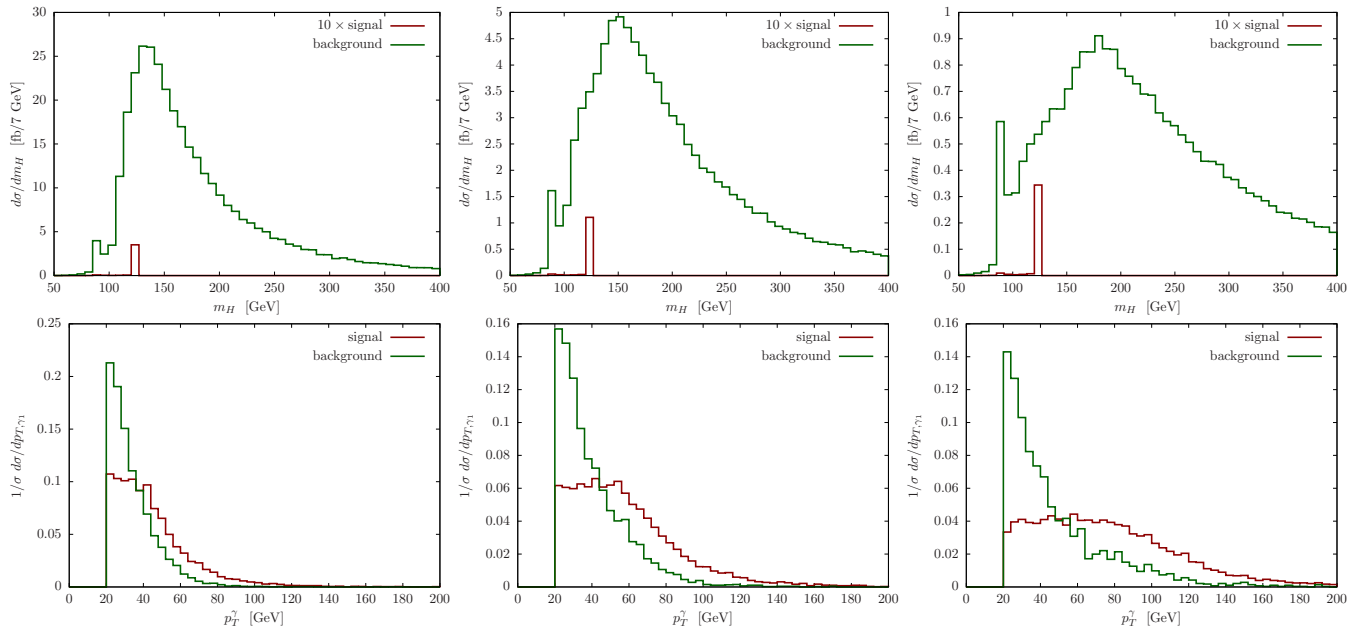


FIG. 1. $m_{\ell\ell\gamma} \equiv m_H$ (top) and $p_T^\gamma$ (bottom) distributions after event selection (for $m_{\ell\ell\gamma}$ the requirement 115 GeV $\leq m_{\ell\ell\gamma} \leq$ 135 GeV is not applied). Distributions are shown for three reference cuts of the transverse momentum of the leading jet: $p_T^{j_1} > 50$ GeV (left), $p_T^{j_1} > 100$ GeV (middle) and $p_T^{j_1} > 180$ GeV (right).

| | | $\sigma_S$ (fb) | $\sigma_B$ (fb) | $S/B$ | $S/\sqrt{B}$ ($\mathcal{L} = 3000$ fb$^{-1}$) |
|---|---|---|---|---|---|
| $p_T^{j_{cut}} = 50$ GeV | Event Selection | 0.424 | 61.515 | 0.0069 | 2.96 |
| | $m_{\ell\ell\gamma} \in [122, 128]$ GeV | 0.408 | 12.243 | 0.033 | 6.39 |
| | $p_T^\gamma \geq 35$ GeV | 0.250 | 4.413 | 0.057 | 6.52 |
| $p_T^{j_{cut}} = 100$ GeV | Event Selection | 0.131 | 10.14 | 0.0129 | 2.25 |
| | $m_{\ell\ell\gamma} \in [122, 128]$ GeV | 0.125 | 1.974 | 0.063 | 4.88 |
| | $p_T^\gamma \geq 40$ GeV | 0.087 | 0.775 | 0.112 | 5.41 |
| $p_T^{j_{cut}} = 180$ GeV | Event Selection | 0.034 | 1.446 | 0.0232 | 1.53 |
| | $m_{\ell\ell\gamma} \in [122, 128]$ GeV | 0.032 | 0.297 | 0.108 | 3.23 |
| | $p_T^\gamma \geq 45$ GeV | 0.024 | 0.120 | 0.203 | 3.86 |

TABLE I. 13 TeV LHC cross section (in fb) for SM signal $\sigma_S$ and background $\sigma_B$ after event selection, Higgs mass window cut $m_{\ell\ell\gamma} \in [122, 128]$ GeV and a further sliding cut on $p_T^\gamma$, respectively for a leading jet transverse momentum cut $p_T^{j_{cut}} = 50$, 100, 180 GeV. The values of signal-to-background $S/B$ and statistical significance $S/\sqrt{B}$ (for $\mathcal{L} = 3000$ fb$^{-1}$) at each stage of the analysis are also shown.

Further SM background suppression may be achieved by imposing a tighter Higgs invariant mass window $m_{\ell\ell\gamma} \in [122, 128]$ GeV in accordance with [3]. As shown in Figure 1, this is more efficient for higher values of $p_T^{j_1}$. In addition, a harder cut on $p_T^\gamma$ correlated with the value of $p_T^{j^{cut}}$ yields a further background reduction, as can be seen from Figure 1 (bottom).

The results in Table I show that requiring the Higgs to be produced in association with a moderately boosted jet, such that $p_T^{j^{cut}} \in [50, 100]$ GeV, significantly improves both $S/B$ and $S/\sqrt{B}$ with respect to the inclusive search. The results also show that the potentially achievable value of $S/B$ increases with larger $p_T^{j^{cut}}$, however at the expense of a lower significance $S/\sqrt{B}$ due to the very small signal cross section at the LHC. A high value $p_T^{j^{cut}} > 100$ GeV would then be particularly helpful if the measurement of $h \to Z\gamma$ at the HL-LHC is systematically limited.

*(ii) Higgs production in weak boson fusion*

We now explore alternative Higgs production modes at the LHC which yield a fairly boosted Higgs boson, together with a not-so-small cross section. These two requirements single out the WBF topology[1], where the Higgs boson recoils against two highly energetic forward jets, as the only alternative to the $h$+jet Higgs production mode analyzed in the previous section. Our signal corresponds to Higgs production in association with two jets, both in WBF and in gluon fusion (GF), while the relevant SM background is $Z\gamma jj$ ($Z \to \ell^+\ell^-$).

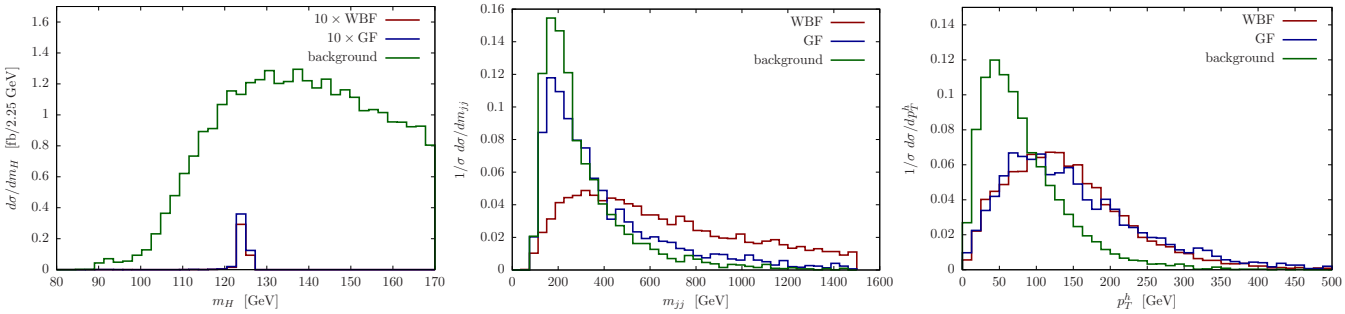


FIG. 2. $m_{\ell\ell\gamma} \equiv m_H$ (left), $m_{jj}$ (middle) and $p_T^{\ell\ell\gamma} \equiv p_T^h$ (right) distributions for signal (WBF and GF) and background after event selection (for $m_{\ell\ell\gamma}$ the selection 115 GeV $\leq m_{\ell\ell\gamma} \leq$ 135 GeV is not imposed).

| | Event Selection | $m_{\ell\ell\gamma} \in [122, 128]$ GeV | $\lvert\Delta y_{jj}\rvert > 3.0$ | $p_T^h > 80$ GeV |
|---|---|---|---|---|
| $\sigma_{\rm WBF}$ (fb) | 0.041 | 0.039 | 0.027 | 0.0208 |
| $\sigma_{\rm GF}$ (fb) | 0.051 | 0.049 | 0.011 | 0.0084 |
| $\sigma_B$ (fb) | 12.168 | 3.753 | 0.373 | 0.1512 |
| $S/B$ | 0.0076 | 0.0236 | 0.102 | 0.193 |
| $S/\sqrt{B}$ (3000 fb$^{-1}$) | 1.44 | 2.51 | 3.40 | 4.11 |

TABLE II. 13 TeV LHC cross section (in fb) in the $\ell^+\ell^-\gamma jj$ final state for WBF signal $\sigma_{\rm WBF}$, GF signal $\sigma_{\rm GF}$ and background $\sigma_B$ after event selection, Higgs mass window cut $m_{\ell\ell\gamma} \in [122, 128]$ GeV and further WBF selection cuts $|\Delta y_{jj}| > 3.0$ and $p_T^h > 80$ GeV. The values of signal-to-background $S/B$ and statistical significance $S/\sqrt{B}$ (for $\mathcal{L} = 3000$ fb$^{-1}$) at each stage of the analysis are also shown.

We adopt the same event generation and event selection criteria as in the previous Section, i.e. $p_T^\ell > 10$ GeV, $|y_\ell| < 2.5$, $p_T^\gamma > 20$ GeV, $|y_\gamma| < 2.5$, as well as the invariant mass windows 80 GeV $\leq m_{\ell\ell} \leq$ 100 GeV, 115 GeV $\leq m_{\ell\ell\gamma} \leq$ 135 GeV. For the $R = 0.4$ anti-$kT$ jets we require $p_T^j \geq 50$ GeV, $|y_j| \leq 4.5$ and $\Delta R_{jj} \geq 2.0$.

[1] We note that $h \to Z\gamma$ in WBF has already been initially studied in [10].

Since NLO QCD corrections to weak boson fusion are known to be relatively small [11, 12], we adopt a $k$-factor $k = 1.0$ for WBF, which we conservatively extend to the (subdominant after cuts) GF signal contribution. Similarly, we use a flat NLO $k$-factor $k = 1.2$ for the SM background [13].

The $m_{jj}$, $p_T^{\ell\ell\gamma} \equiv p_T^h$ and $m_{\ell\ell\gamma}$ distributions (the latter without imposing 115 GeV $\leq m_{\ell\ell\gamma} \leq$ 135 GeV) after event selection for WBF, GF and the background are shown in Figure 2. To improve our signal sensi-

tivity we further require a tight Higgs mass window $m_{\ell\ell\gamma} \in [122, 128]$ GeV as well as WBF selection cuts[2] $|\Delta y_{jj}| > 3.0$ and $p_T^h > 80$ GeV. The results for $S/B$ and $S/\sqrt{B}$ are shown in Table II, where it becomes clear that WBF does not perform as well as $h$+jet in terms of sensitivity to $h \to Z\gamma$. Still, a hypothetical combination of sensitivities between $h$+jet and WBF Higgs production (we perform a naive combination in quadrature) could yield $S/\sqrt{B} \sim 7.7$, improving over the $h$+jet alone.

### $h \to Z\gamma$ at Future $e^+e^-$ Colliders

We now explore the sensitivity to the decay $h \to Z\gamma$ that could be obtained for a future $e^+e^-$ collider. We focus on a circular $e^+e^-$ collider (hereinafter *fcc-ee*) in two configurations: a c.o.m. energy of $\sqrt{s} = 240$ GeV, with a projected integrated luminosity of 10 ab$^{-1}$ [14], and a c.o.m. energy of $\sqrt{s} = 350$ GeV, with a projected integrated luminosity of 2.6 ab$^{-1}$ [14]. The Higgs production process considered is $e^+e^- \to Zh$, which has the highest cross section for an $e^+e^-$ collider with the chosen c.o.m. As compared to LHC, searches for $h \to (Z \to \ell^+\ell^-)\gamma$ at *fcc-ee* take advantage of the large amount of integrated luminosity as well as the presence of the extra $Z$ boson in the process. In order to maximize the sensitivity, we jointly consider the final states[3] $Z \to jj$, $\ell^+\ell^-$ for the extra $Z$ boson. The dominant SM background is the irreducible $e^+e^- \to ZZ\gamma$, with $ZZ \to 2\ell\,2j$, $4\ell$.

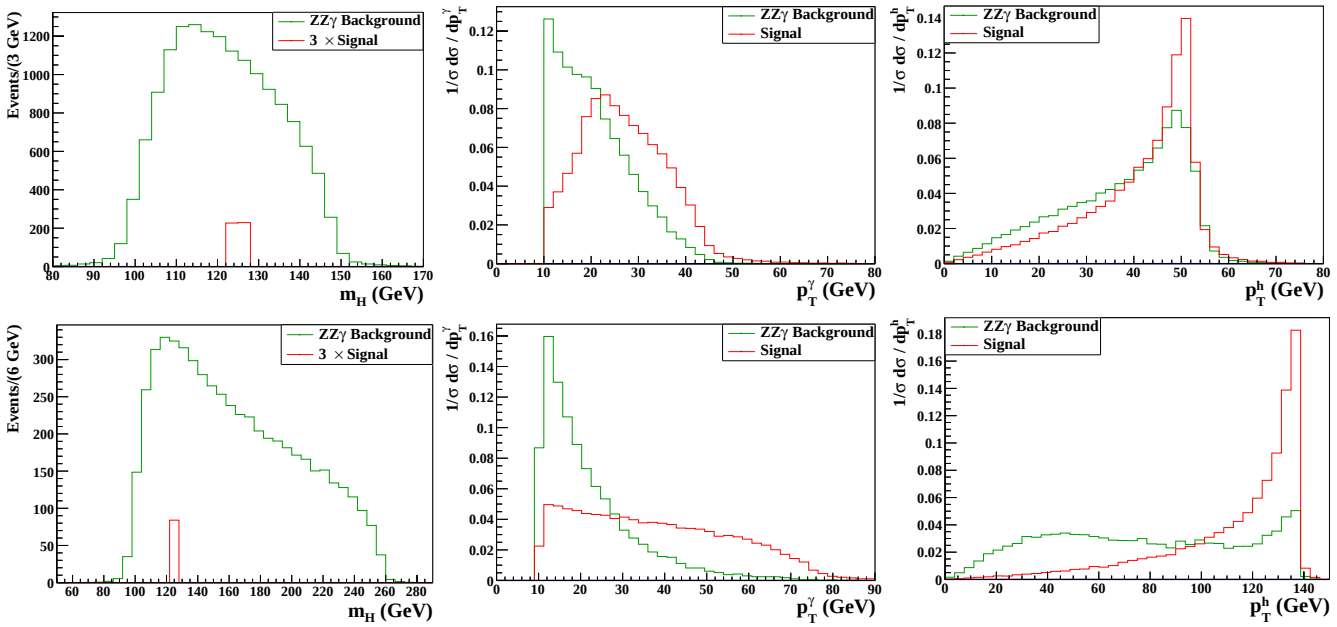


FIG. 3. Signal and background distributions for *fcc-ee* $\sqrt{s} = 240$ GeV (top) and $\sqrt{s} = 350$ GeV (bottom) after event selection: $m_{\ell\ell\gamma} \equiv m_H$ (left) without imposing the selection 115 GeV $\leq m_{\ell\ell\gamma} \leq$ 135 GeV. $p_T^\gamma$ (middle) after requiring $m_{\ell\ell\gamma} \in [122, 128]$ GeV. $p_T^{\ell\ell\gamma} \equiv p_T^h$ (right) after requiring $m_{\ell\ell\gamma} \in [122, 128]$ GeV.

| | | $\sigma_S$ (fb) | $\sigma_B^{ZZ\gamma}$ (fb) | $S/B$ | $S/\sqrt{B}$ |
|---|---|---|---|---|---|
| $\sqrt{s} = 240$ GeV ($\mathcal{L} = 10$ ab$^{-1}$) | Event Selection | 0.0154 | 1.542 | 0.01 | 1.24 |
| | $m_{\ell\ell\gamma} \in [122, 128]$ GeV | 0.0154 | 0.220 | 0.07 | 3.28 |
| | $p_T^\gamma > 20$ GeV | 0.0116 | 0.103 | 0.113 | 3.62 |
| $\sqrt{s} = 350$ GeV ($\mathcal{L} = 2.6$ ab$^{-1}$) | Event Selection | 0.0107 | 2.123 | 0.005 | 0.37 |
| | $m_{\ell\ell\gamma} \in [122, 128]$ GeV | 0.0107 | 0.125 | 0.086 | 1.54 |
| | $p_T^\gamma > 20$ GeV, $p_T^h > 90$ GeV | 0.0071 | 0.020 | 0.354 | 2.56 |

TABLE III. *fcc-ee* cross section for signal and background after event selection, Higgs mass window cut $m_{\ell\ell\gamma} \in [122, 128]$ GeV and further selection cuts $p_T^\gamma > 20$ GeV, $p_T^h > 90$ GeV. Values of $S/B$ and $S/\sqrt{B}$ at each stage of the analysis are also shown.

[2] After these two cuts, a potential $m_{jj} > 300$ GeV cut has only a mild impact on $S/B$.

[3] The $Z \to \nu\bar{\nu}$ final state suffers from the large SM background $e^+e^- \to W^+W^-\gamma$ ($W^+W^- \to 2\ell\,2\nu$), and thus we do not consider it here. Still, its addition could mildly improve the sensitivity to $h \to Z\gamma$.

We consider unpolarized $e^+e^-$ beams [14, 15], and as in the previous Section we generate the signal and background with MadGraph_aMC@NLO and shower the partonic process with Pythia 8. For event selection we require for the leptons $p_T^\ell > 10$ GeV, $|y_\ell| < 2.5$, for the photon $p_T^\gamma > 10$ GeV, $|y_\gamma| < 2.5$, and for the jets (for $Z \to jj$) $p_T^j > 20$ GeV and $|y_j| < 5$, and further require $m_{\ell\ell} \in [80,\ 100]$ GeV, $m_{jj} \in [80,\ 100]$ GeV.

The cross section for the signal $e^+e^- \to Zh$ is $\sigma_{Zh} = 0.193$ pb ($\sigma_{Zh} = 0.132$ pb) for $\sqrt{s} = 240$ GeV ($\sqrt{s} = 350$ GeV). After the decay $h \to \ell^+\ell^-\gamma$ we then expect $\sim 154$ signal events with $\mathcal{L} = 10$ ab$^{-1}$ for $\sqrt{s} = 240$ GeV, and $\sim 28$ signal events with $\mathcal{L} = 2.6$ ab$^{-1}$ for $\sqrt{s} = 350$ GeV, which means that tight cuts are not helpful in extracting the signal due to the very small cross section. Cross sections for the SM signal and background after event selection are shown in Table III. As in the previous Section, we define our Higgs mass signal region as $m_{\ell\ell\gamma} \in [122, 128]$ GeV. In order to further increase $S/B$ in the signal region we require $p_T^\gamma > 20$ GeV (for $\sqrt{s} = 240$, 350 GeV), together with $p_T^h > 90$ GeV (only for $\sqrt{s} = 350$ GeV). The invariant mass distribution $m_{\ell\ell\gamma}$ as well as the $p_T^\gamma$ and $p_T^h$ distributions in the signal region are shown in Figure 3.

The results in Table III show that, while the values of $S/B$ achievable by a future *fcc-ee* machine in the measurement of $h \to Z\gamma$ may be higher than those of LHC (for $\sqrt{s} = 350$ GeV), a precise measurement at *fcc-ee* is limited by statistics, and the projected signal significance at the HL-LHC in the $h$+jet production channel is significantly larger.

### Probing New Physics with $h \to Z\gamma$

Precisely measuring the 125 GeV Higgs boson signal strengths in the $h \to Z\gamma$ and $h \to \gamma\gamma$ final states could reveal the existence of new charged particles coupled to $h$ (see e.g. [16, 17]). While the results of the above sections show that a precise measurement of the signal strength for $h \to Z\gamma$ is possible at the LHC (and to a lesser extend, at a future *fcc-ee* collider), the achieved precision in the measurement of the $h \to \gamma\gamma$ signal strength will be much higher in both colliders, and as such new charged particles coupled to the Higgs would first manifest themselves via a deviation in the $h \to \gamma\gamma$ channel w.r.t. the SM value. Still, the precise measurement of the $h \to Z\gamma$ signal strength would yield valuable complementary information to the $h \to \gamma\gamma$ channel, regarding the $SU(2)_{\rm L} \times U(1)_{\rm Y}$ quantum numbers of these new charged particles.

Let us consider the partial widths $\Gamma(h \to \gamma\gamma) \equiv \Gamma_{\gamma\gamma}$ and $\Gamma(h \to Z\gamma) \equiv \Gamma_{Z\gamma}$ in the presence of a BSM contribution encoded in the effective operators

$$\kappa_B \frac{\alpha_{\rm EM}}{8\pi v\, c_W^2} B_{\mu\nu} B^{\mu\nu} \quad , \quad \kappa_W \frac{\alpha_{\rm EM}}{8\pi v\, s_W^2} W^a_{\mu\nu} W_a^{\mu\nu} \,. \qquad (1)$$

with $s_W$ ($c_W$) being the sine (cosine) of the Weinberg angle. The partial widths read

$$\Gamma_{\gamma\gamma} = \frac{\alpha_{\rm EM}^2 m_h^3}{256\,\pi^3 v^2} \left| \kappa_W + \kappa_B + A_1(\tau_W) + \sum_f 3 Q_f^2 A_{1/2}(\tau_f) \right|^2 \qquad (2)$$

$$\Gamma_{Z\gamma} = \frac{\alpha_{\rm EM}^2 m_h^3}{128\,\pi^3 v^2} \left(1 - \frac{m_Z^2}{m_h^2}\right)^3 \left| t_W^{-1} \kappa_W - t_W \kappa_B + \frac{A_1(\tau_W, \lambda_W)}{s_W} + \sum_f 3 \frac{Q_f (2 I_f^3 - 4 Q_f s_W^2)}{s_W c_W} A_{1/2}(\tau_f, \lambda_f) \right|^2 \qquad (3)$$

with $Q_f$ and $I_f^3$ the electric charge and third component of weak isospin of the SM fermions $f$ entering the $h \to \gamma\gamma$ and $h \to Z\gamma$ loops. The form factors $A_1(x)$, $A_{1/2}(x)$, $A_1(x, y)$, $A_{1/2}(x, y)$ are given in [18], with $\tau_i = m_h^2/(4m_i^2)$ and $\lambda_i = m_Z^2/(4m_i^2)$.

For $h \to \gamma\gamma$, Higgs signal strength measurements with 7 - 8 TeV LHC data yield a signal strength value $\mu_{\gamma\gamma} = 1.17 \pm 0.27$ [19]. For 14 TeV LHC with 3000 fb$^{-1}$ the projected signal strength sensitivity is $\Delta\mu_{\gamma\gamma} = 0.04$ [4]. From the present analysis, for the HL-LHC with 3000 fb$^{-1}$ the projected signal strength sensitivity in $h \to Z\gamma$ (combining the results from $h$+jet and WBF Higgs production) is $\Delta\mu_{Z\gamma} \simeq 0.13$ neglecting systematic uncertainties ($\Delta\mu_{Z\gamma} \simeq 0.2$ considering the same amount of systematics as in [3]). In order to illustrate the potential gain of studying the decays $h \to \gamma\gamma$ and $h \to Z\gamma$ in concert, let us consider two alternative hypothetical scenarios:

*(i)* No deviation in $\mu_{\gamma\gamma}$ and $\mu_{Z\gamma}$ w.r.t. to the SM is measured at the HL-LHC.

*(ii)* A deviation in $\mu_{\gamma\gamma}$ w.r.t. to the SM is measured at the HL-LHC. We choose $\mu_{\gamma\gamma} = 1.17$ (corresponding to the LHC Run 1 central value for the signal strength), and consider three possible measured values $\mu_{Z\gamma} = 0.5$, 0.65, 0.8 at the HL-LHC.

In these two scenarios, we then show in Figure 4 the would-be 95 % C.L. limits in the ($\kappa_W$, $\kappa_B$) plane from a $\chi^2$ fit (assuming for simplicity no systematic uncertainties in the HL-LHC measurement of $\mu_{Z\gamma}$). For scenario

*(i)* (Figure 4, Top) the combination of $\mu_{\gamma\gamma}$ and $\mu_{Z\gamma}$ constrains a blind direction (present for $\mu_{\gamma\gamma}$ only) in the ($\kappa_W$, $\kappa_B$) plane, limiting $\kappa_B$ to the range $[-1.18, 1.29]$ and $\kappa_W$ to the range $[-0.93, 1.02]$ at 95 % C.L. For scenario *(ii)* (Figure 4, Bottom), the combination of $\mu_{\gamma\gamma}$ and $\mu_{Z\gamma}$ allows to extract bounds on the $SU(2)_{\rm L}\times U(1)_{\rm Y}$ properties of the would-be charged particle(s) responsible for the signal strength deviations. The ratio $\kappa_B/\kappa_W$ is given by

$$\frac{\kappa_B}{\kappa_W} \equiv \tan(\Theta) = \frac{12\,{\rm Y}^2}{(N-1)(N+1)} \qquad (4)$$

where Y is the hypercharge of the new charged particle and $N = 1, 2, 3, 4...$ denotes its $SU(2)_{\rm L}$ representation ($1$ = singlet, $2$ = doublet, $3$ = triplet...). The notation $\kappa_B/\kappa_W = \tan(\Theta)$ has been introduced for convenience (see e.g. [20]). The measurements $\mu_{Z\gamma} = 0.5, 0.65, 0.8$ respectively yield the bounds $\Theta \in [2.40, 3.53]$, $\Theta \in [2.41, 4.7]$, $\Theta \in [2.44, 5.18]$ at 95 % C.L. and in the first case the $SU(2)_{\rm L}$ singlet hypothesis ($\Theta = \pi/2, 3\pi/2$) would be disfavoured at more than $2\sigma$ by means of the combined $\mu_{Z\gamma}$, $\mu_{\gamma\gamma}$ measurement.

Before concluding, it is also important to stress that the $h \to Z\gamma$ decay is also a potential window into new physics in other contexts: Interference effects involving $h \to Z\gamma$ have been studied in [21–24] as a future probe of the CP properties of the 125 GeV Higgs boson, and improving the sensitivity to $h \to Z\gamma$ could also improve some of these measurements. Similarly, precise measurements of $h \to Z\gamma$ would also allow to constrain the presence of light pseudoscalars $a$ to which the Higgs can decay (via $h \to Z\,a$), for a dominant pseudoscalar decay $a \to \gamma\gamma$ (see e.g. [25, 26]) with two very collimated photons (which do not get resolved in the detector).

## Conclusions

The decay $h \to Z\gamma$ is very challenging to measure precisely at the LHC or a future $e^+e^-$ collider. In this work we have shown that considering Higgs production in association with a moderately boosted jet at the LHC can significantly improve the sensitivity in this channel compared to the inclusive measurement, due to kinematic (de)correlations among $p_T^j$, $m_{\ell\ell\gamma}$ and $p_T^\gamma$ for signal and background in the $\ell\ell\gamma+j$ final state. By combining these measurements with those of $h \to Z\gamma$ in the (less sensitive) weak boson fusion Higgs production channel, we show that it could be possible to achieve $\Delta\mu_{Z\gamma} \sim 0.13$ (in the absence of systematic uncertainties) at the HL-LHC with $\mathcal{L} = 3000$ fb$^{-1}$. We have also illustrated the potential of such a measurement to probe new physics scenarios, particularly to gain information on the $SU(2)\times U(1)$ quantum numbers of would-be charged particles coupled to the Higgs.

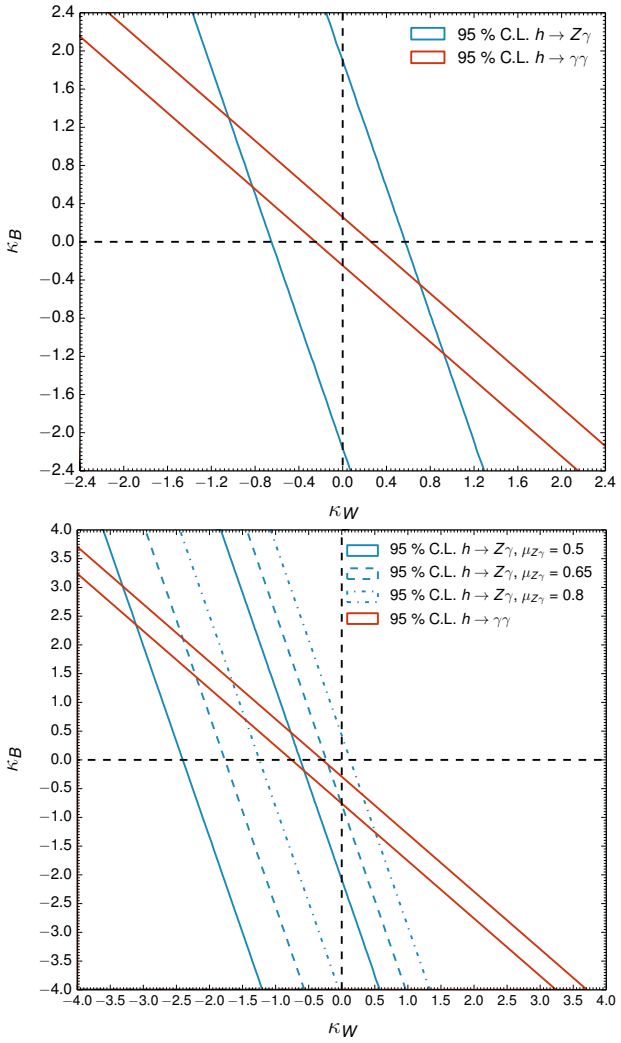
95 % C.L. $h \to Z\gamma$
95 % C.L. $h \to \gamma\gamma$
$\kappa_B$
$\kappa_W$
95 % C.L. $h \to Z\gamma$, $\mu_{Z\gamma}$ = 0.5
95 % C.L. $h \to Z\gamma$, $\mu_{Z\gamma}$ = 0.65
95 % C.L. $h \to Z\gamma$, $\mu_{Z\gamma}$ = 0.8
95 % C.L. $h \to \gamma\gamma$
$\kappa_B$
$\kappa_W$

FIG. 4. 95 % C.L. bounds in the ($\kappa_W$, $\kappa_B$) plane from measurements of Higgs signal strengths $\mu_{\gamma\gamma}$ (red) and $\mu_{Z\gamma}$ (blue) at HL-LHC. Top: Assuming measured central values $\mu_{\gamma\gamma} = 1$, $\mu_{Z\gamma} = 1$ (no deviations from SM). Bottom: Assuming measured central values $\mu_{\gamma\gamma} = 1.17$ and $\mu_{Z\gamma} = 0.5, 0.65, 0.8$, respectively solid, dashed, dot-dashed.

Finally, it is important to stress that the $h \to Z\gamma$ measurement strategy in $h$+jet discussed here, while yielding fair precision at the HL-LHC, could be optimally exploited at a 100 TeV *fcc-pp* due to the much higher $h$+jet cross section (particularly at high $p_T^j$), allowing for a very strong background suppresion without being statistically limited by the small LHC cross sections.

## Acknowledgements

J.M.N. is supported in part by the People Programme (Marie Curie Actions) of the European Union Seventh Framework Programme (FP7/2007-2013), REA grant agreement PIEF-GA-2013-625809 and the European Research Council under the European Unions Horizon 2020 program (ERC Grant Agreement no.648680 DARK-

HORIZONS). M.S. is supported in part by the European Commission through the "HiggsTools" Initial Training Network PITN-GA-2012-316704.

[1] S. Chatrchyan *et al.* [CMS Collaboration], Phys. Lett. B **726**, 587 (2013) [arXiv:1307.5515 [hep-ex]].
[2] G. Aad *et al.* [ATLAS Collaboration], Phys. Lett. B **732**, 8 (2014) [arXiv:1402.3051 [hep-ex]].
[3] ATLAS-PHYS-PUB-2014-006
[4] ATLAS-PHYS-PUB-2014-016
[5] J. Alwall *et al.*, JHEP **1407**, 079 (2014) [arXiv:1405.0301 [hep-ph]].
[6] T. Sjostrand, S. Mrenna and P. Z. Skands, Comput. Phys. Commun. **178**, 852 (2008) [arXiv:0710.3820 [hep-ph]].
[7] F. Caola, S. Forte, S. Marzani, C. Muselli and G. Vita, JHEP **1608**, 150 (2016) [arXiv:1606.04100 [hep-ph]].
[8] D. de Florian *et al.* [LHC Higgs Cross Section Working Group Collaboration], arXiv:1610.07922 [hep-ph].
[9] J. M. Campbell, H. B. Hartanto and C. Williams, JHEP **1211**, 162 (2012) [arXiv:1208.0566 [hep-ph]].
[10] ATLAS-PHYS-PUB-2013-014
[11] T. Figy, C. Oleari and D. Zeppenfeld, Phys. Rev. D **68**, 073005 (2003) [hep-ph/0306109].
[12] M. Cacciari, F. A. Dreyer, A. Karlberg, G. P. Salam and G. Zanderighi, Phys. Rev. Lett. **115**, no. 8, 082002 (2015) [arXiv:1506.02660 [hep-ph]].
[13] F. Campanario, M. Kerner, L. D. Ninh and D. Zeppenfeld, Eur. Phys. J. C **74**, no. 9, 3085 (2014) [arXiv:1407.7857 [hep-ph]].
[14] M. Bicer *et al.* [TLEP Design Study Working Group Collaboration], JHEP **1401**, 164 (2014) [arXiv:1308.6176 [hep-ex]].
[15] S. R. Mane, arXiv:1406.0561 [physics.acc-ph].
[16] C. W. Chiang and K. Yagyu, Phys. Rev. D **87**, no. 3, 033003 (2013) [arXiv:1207.1065 [hep-ph]].
[17] M. Carena, I. Low and C. E. M. Wagner, JHEP **1208**, 060 (2012) [arXiv:1206.1082 [hep-ph]].
[18] A. Djouadi, Phys. Rept. **457**, 1 (2008) [hep-ph/0503172].
[19] G. Aad *et al.* [ATLAS Collaboration], Eur. Phys. J. C **76**, no. 1, 6 (2016) [arXiv:1507.04548 [hep-ex]].
[20] R. Sato and K. Tobioka, Phys. Lett. B **760**, 590 (2016) [arXiv:1605.05366 [hep-ph]].
[21] A. Y. Korchin and V. A. Kovalchuk, Phys. Rev. D **88**, no. 3, 036009 (2013) [arXiv:1303.0365 [hep-ph]].
[22] Y. Chen, R. Harnik and R. Vega-Morales, Phys. Rev. Lett. **113**, no. 19, 191801 (2014) [arXiv:1404.1336 [hep-ph]].
[23] Y. Chen, A. Falkowski, I. Low and R. Vega-Morales, Phys. Rev. D **90**, no. 11, 113006 (2014) [arXiv:1405.6723 [hep-ph]].
[24] M. Farina, Y. Grossman and D. J. Robinson, Phys. Rev. D **92**, no. 7, 073007 (2015) [arXiv:1503.06470 [hep-ph]].
[25] K. Mimasu and V. Sanz, JHEP **1506**, 173 (2015) [arXiv:1409.4792 [hep-ph]].
[26] J. Jaeckel and M. Spannowsky, Phys. Lett. B **753**, 482 (2016) [arXiv:1509.00476 [hep-ph]].